# A Priori Phase Prediction of Zeolites: Case Study of the Structure-Directing Effects in the Synthesis of MTT-Type Zeolites

Allen W. Burton

*Contribution from the Chevron Energy Technology Company, Richmond, California 94802*

Received January 23, 2007; E-mail: buaw@chevron.com

**Abstract:** This study first uses molecular modeling to examine the structure-directing effects of small amines that are selective for the crystallization of **MTT**-type zeolite phases. The optimized van der Waals interactions of these small amines are compared within the one-dimensional pore zeolites with the **MTT**, **TON**, and **MTW** frameworks. From these results and our previous molecular modeling studies of structure-directing agents (SDA) for **MTT**-type zeolites, a large number of amines or quaternary ammonium molecules are successfully predicted to be selective for **MTT** phases. These molecules were chosen by matching the crystallographic periodicity of the pore structure with the distances between the centers of branched groups in these molecules. These molecules vary in length and in the number of branched moieties, and a few of these molecules are polymeric or oligomeric. In test cases where the distances between the branched groups are not multiples of the pore periodicity, with few exceptions these molecules usually do not produce **MTT** phases. Finally, we discuss the inorganic conditions necessary for crystallization of **MTT** phases in borosilicate preparations with some of the diamines in this investigation.

## I. Introduction

Zeolites are an important class of crystalline microporous materials with industrial applications in ion exchange, adsorption, and catalysis. High-silica zeolites are particularly vital in the synthesis of petrochemicals and refining of petroleum.[1−6] They are used as solid acid catalysts in the alkylation of benzene to cumene and ethylbenzene,[7,8] the isomerization of xylene,[8] and the transalkylation of aromatics (e.g., toluene disproportionation).[8,9] Siliceous zeolites are essential additives in modern catalytic cracking units,[10,11] and they are also used to reduce the pour point in motor lubricant stocks either by selective cracking or by selective isomerization of long-chain paraffins.[3,12,13]

For over half a century, zeolites have been synthesized in industrial and academic laboratories. Despite their widespread use as catalysts, we still do not fundamentally understand the mechanisms of self-assembly that determine which zeolite phases are promoted under a given set of synthesis conditions. Both the inorganic and organic (typically an amine or quaternary ammonium compound) components of a synthesis gel influence the zeolite phases that may crystallize. Since the organic species are a strong determinant of the phases that are crystallized, they are often referred to as "structure-directing agents" (SDAs).

It is important to appreciate that zeolites are metastable phases. For identical gel compositions with the same SDA, changes in temperature, hydroxide concentration, or sources of inorganic reactants or even the presence of seeds may influence the phase that is crystallized. Furthermore, Ostwald ripening may occur in which a zeolite phase converts to either a more thermodynamically favored zeolite phase or a dense silica phase such as quartz. Because crystallization products from zeolite syntheses are kinetically driven, a hypothetical SDA/zeolite composite that represents a thermodynamic minimum (when compared to the same SDA within other zeolite frameworks) may not necessarily crystallize in a given system.

However, Sastre et al. reasoned that the relative stabilities of potentially competing nuclei may "give us an estimation of which zeolite is preferentially forming during the early stages of the synthesis."[14] In this simplified treatment, by assuming that the structures of competing nuclei resemble the structures of their respective SDA/framework composites, we can approximate the relative energies of those competing nuclei. This reasoning is similar to that presented by the late Barrie Lowe, who suggested that nuclei with greater free energy are more

(1) *Zeolites for Cleaner Technologies*; Guisnet, M., Gilson, J.-P., Eds.; Imperial College: London 2002.
(2) Weitkamp, J.; Puppe, L. *Catalysis and Zeolites: Fundamentals and Applications*; Springer: New York 1999.
(3) Degnan, T. *Top. Catal.* **2000**, *13*, 349−356.
(4) Chen, N. Y. *Shape Selective Catalysis in Industrial Applications*; Marcel Dekker: New York 1996.
(5) Corma, A. *Catal. Lett.* **1993**, *22*, 33−52.
(6) Bhatia, S. *Zeolite Catalysis: Principles and Applications*; CRC Press: Boca Raton, FL, 1990.
(7) Perego, C.; Ingallina, P. *Catal. Today* **2002**, *23*, 3−22.
(8) Cejka, J.; Wichterlova, B. *Catal. Rev.* **2002**, *44*, 375−421.
(9) Tsai, T.-C.; Liu, S.-B.; Wang, I. *Appl. Catal. A: Gen.* **1999**, *181*, 355−398.
(10) Scherzer, J. *Octane-Enhancing Zeolite FCC Catalysts: Scientific and Technical Aspects*; Marcel Dekker: New York, 1990.
(11) *Fluid Cracking Catalysts*; Occelli, M., O'Connor, P., Eds.; Marcel Dekker: New York, 1998.
(12) Sivasanker, S. *Bull. Catal. Soc. India* **2003**, *2*, 100−106.
(13) Miller, S. U.S. Patent 5135638, 1992.

(14) Sastre, G.; Leiva, S.; Sabater, M. J.; Gimenez, I.; Rey, F.; Valencia, S.; Corma, A. *J. Phys. Chem. B* **2003**, *107* (23), 5432−5440.
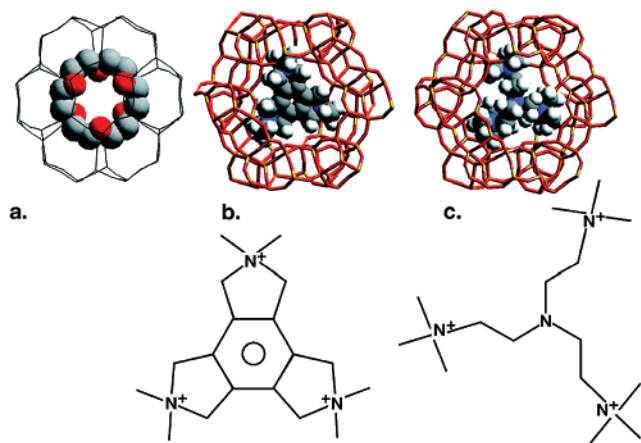
**Figure 1.** (a) 18-Crown-6 molecule enclathrated within the 18 ring cages of MCM-61 and Mu-13 (only oxygen and carbon atoms shown (from ref 20). (b) Triquat 2 within the **MEI** cage. (c) Triquat 2 within the **MEI** cage. C, N, O, and H atoms are represented by gray, blue, red, and white spheres, respectively.

likely to redissolve than to participate in crystallization.[15] Although a phase predicted to be thermodynamically favored does not always crystallize, we can say that it is more probable that a phase will form if it is energetically favored. This is borne out by the fact that there is a "good" calculated fit for many observed SDA/framework composites, especially in cases where a particular siliceous framework is rarely or never observed to crystallize with other SDA molecules (vide infra). In previous work we identified three major contributions to the energy of an SDA/framework composite: the inherent energy of the defect-free framework, the interactions between the SDA and the framework (in which we include the conformational energy of the occluded SDA relative to the minimum energy conformation), and the concentration of silanol/siloxy defects in the final product.[16] In general, defect-free zeolite structures with similar framework density tend to have similar framework energies.[17,18] If the concentration of silanol/siloxy defects (due to a greater concentration of extraframework charge relative to the concentration of framework aluminum) is similar in two zeolites with similar framework densities, then the relative energies of the two phases will largely be determined by the interactions between the SDA and the respective frameworks. In this respect, molecular modeling is useful for examining the structure-directing effects of known molecules as well as predicting candidate SDA molecules for a given zeolite structure.

Excellent examples of structure direction are the 18-Crown-6 molecules in the synthesis of MCM-61 (and its aluminophosphate analogue Mu-13) and the triquaternary ammonium (triquat) molecule used in the synthesis of ZSM-18.[19] In both cases the size and symmetry of the molecules are reflected in the cages within which they are occluded (Figure 1a−c). The aluminosilicate MCM-61[20] and the aluminophosphate Mu-13[21] both possess the **MSO** framework. The three-letter code indicates a

unique zeolite framework topology assigned by the Structure Commission of the International Zeolite Association. The Appendix in the Supporting Information contains images of all the frameworks discussed in this paper. Although there are several examples of zeotype frameworks that may be prepared in both aluminosilicate and aluminophosphate forms, they are rarely prepared using SDAs with identical backbone structures. The case of MCM-61 and Mu-13 is therefore a very notable example of structure direction.

After we determine the zeolite phases that are directed by a particular organic, we frequently perform molecular modeling to show, a posteriori, that there is a good energetic fit of the molecule within the host framework. Despite the existence of powerful computing algorithms[22−24] for building SDA molecules within zeolite void spaces, rarely in the literature do we find examples in which a previously unstudied molecule is accurately predicted to crystallize a particular zeolite. Such predictions often require that an unusual or dominant feature in the zeolite be consistent with the size and shape of the proposed molecule.

The first definitive example of this occurred when Schmitt and Kennedy used molecular modeling to identify candidate molecules to replace the triquat shown in Figure 1b as an SDA for ZSM-18.[25] In this example the investigators sought a molecule that possessed the same charge as well as a similar size and symmetry as the first SDA found to make ZSM-18. This led them to consider the trisquaternary molecule shown in Figure 1c. Using this molecule they were able to prepare samples of ZSM-18 that could be calcined to remove the organic without loss of crystallinity (as they had observed with the first triquat).

Recently Casci and co-workers used molecular modeling to identify the C5-N,N′-bis(1-methylpyrrolidinium) diquat as a candidate for the synthesis of NES-type zeolites.[26] Sastre and co-workers also recently successfully applied molecular modeling to find an SDA that was selective for ITQ-7 (ISV) rather than the structurally similar ITQ-17 (BEC).[27] To that point, only one other SDA had been reported to crystallize ITQ-7. ITQ-17, on the other hand, crystallizes from germanosilicate compositions in the presence of several different quaternary ammonium molecules. Their study was motivated by the fact that the precursor amine used to prepare the previously discovered SDA for ITQ-7 is no longer commercially available.

Another example of a priori zeolite phase prediction involves the synthesis of ITQ-24. In their studies using cyclohexylpyrrolidine derivatives, Rey and co-workers found that one of their diquaternary SDAs promoted the synthesis of ITQ-23 in gels with Si/Al = 50 to θ.[28] ITQ-23 belongs to the SSZ-26/33 intergrowth family of zeolites described by Lobo et al.[29] In the structure elucidation of these zeolites, Lobo described the 26/

(15) Lowe, B. M. *Zeolites* **1983**, *3* (4), 300−305.
(16) Burton, A. W.; Lee, G. S.; Zones, S. I. *Microporous Mesoporous Mater.* **2006**, *90* (1−3), 129−144.
(17) Piccione, P.; Yang S.; Navrotsky, A.; Davis, M. *J. Phys. Chem. B* **2002**, *106* (14), 3629−3638.
(18) Henson, N. J.; Cheetham, A. K.; Gale, J. D *Chem. Mater.* **1998**, *10*, 3966.
(19) Ciric, J. U.S. Patent 3,950,496, 1976.
(20) Shantz, D. F.; Burton, A.; Lobo, R. F. *Microporous Mesoporous Mater.* **1999**, *31*, 61−73.
(21) Paillaud, J.-L.; Caullet, P.; Schreyeck, L.; Marler, B. *Microporous Mesoporous Mater.* **2001**, *42*, 177−189.

(22) Lewis, D. W.; Willock, D. J.; Catlow, C. R. A.; Thomas, J. M.; Hutchings, G. J. *Nature* **1996**, *382*, 604.
(23) Lewis, D. W.; Sankar, G.; Wyles, J.; Thomas, J. M.; Catlow, C. R. A.; Willock, D. J. *Angew. Chem.* **1997**, *36*, 2675.
(24) Willock, D. J.; Lewis, D. W.; Catlow, C. R. A.; Hutchings, G. J.; Thomas, J. M. *J. Mol. Catal. A* **1997**, *119*, 415−424.
(25) Schmitt, K.; Kennedy, G. *Zeolites* **1994**, *14*, 635.
(26) Casci, J. L.; Cox, P. A.; Henney, R. P. G.; Maberly, S.; Shannon, M. D. *Book of Abstracts*, Proceedings of the 14th International Zeolite Conference, Cape Town, South Africa; The Catalysis Society of South Africa: 2004; p 109.
(27) Sastre, G.; Cantin, A.; Diaz-Cabanas, M. J.; Corma, A. *Chem. Mater.* **2005**, *17* (3), 545−552.
(28) Leiva, S.; Gimenez, I.; Corma, A.; Rey, F.; Sabater, M.; Sastre, J. *Book of Abstracts*, Proceedings of the 14th International Zeolite Conference, Cape Town, South Africa; The Catalysis Society of South Africa: 2004; p 265.
(29) Lobo, R. F.; Pan, M.; Chan, I.; Medrud, R. C.; Zones, S. I.; Crozier, P. A.; Davis, M. E. *J. Phys. Chem.* **1994**, *98* (46), 12040−12052.

33 family as a random intergrowth of two polytypes whose relationship is similar to that of the pure polytypes A and B of zeolite beta. Lobo also described a third hypothetical polytype C that possesses double four-ring units in its framework. From their previous work with germanosilicate gels, Corma et al. knew that the presence of germanium favors formation of double four-ring units. A previous publication showed that germanium promoted formation of beta type C (a beta polytype with a high density of double four rings) in systems that otherwise formed conventional zeolite beta when germanium is absent.[30] Since the pore dimensions and distances between channel intersections are similar in polytypes A, B, and C (and therefore the organic should have similar interactions with the framework), Rey et al. speculated that inclusion of germanium should promote the synthesis of the polytype C in this system. Their experiments with germanium indeed led to the synthesis of ITQ-24,[31] which possesses the framework of the previously unobserved polytype C.[32]

In the present study we examine the design of SDA molecules for the syntheses of zeolites with the **MTT** framework topology. This framework is shared by zeolites ZSM-23, KZ-1, EU-13, ISI-6, and SSZ-32. ZSM-23 was first discovered in 1976 by researchers at Mobil using pyrrolidine as an SDA.[33] Later Moini reported that ZSM-23 could be prepared using C7-, C8-, C11-, and C12-trimethylammonium (TMA) diquats.[34] In this context the number after C signifies the carbon length of the methylene chain between the trimethylammonium centers. In 1982 Parker and Bibby reported the crystallization of KZ-1 from aluminosilicate gels (Si/Al > 55) in the presence of pyrrolidine, isopropylamine, or dimethylamine.[35] EU-13 was reported to crystallize from gels containing tetramethylammonium and rubidium.[36] SSZ-32 was synthesized by workers at Chevron using the *N,N′*-diisopropylimidazolium (DIPI) and the *N*-isopropyl-*N′*-methylimidazolium cations as SDAs.[37] Nakagawa subsequently discovered that SSZ-32 could be prepared using isobutylamine, trimethylamine, and diisobutylamine.[38] SSZ-32 can be made with lower Si/Al ratios than the other **MTT** phases. What features do most of these molecules have in common that lend themselves to the synthesis of **MTT**-type zeolites?

We first address this question by performing a series of molecular modeling calculations to examine the optimal packing arrangements of some of the aforementioned molecules in the **MTT** framework. From these energy minimization calculations and from crystallographic considerations of the zeolite framework host we are able to understand the determinant features of the SDA molecules that specify **MTT**-type phases. On the basis of these considerations, we can predict a large family of previously unexamined molecules of varying carbon lengths and shapes that should also yield **MTT**-type phases. For this study we synthesized many of these novel molecules (others are
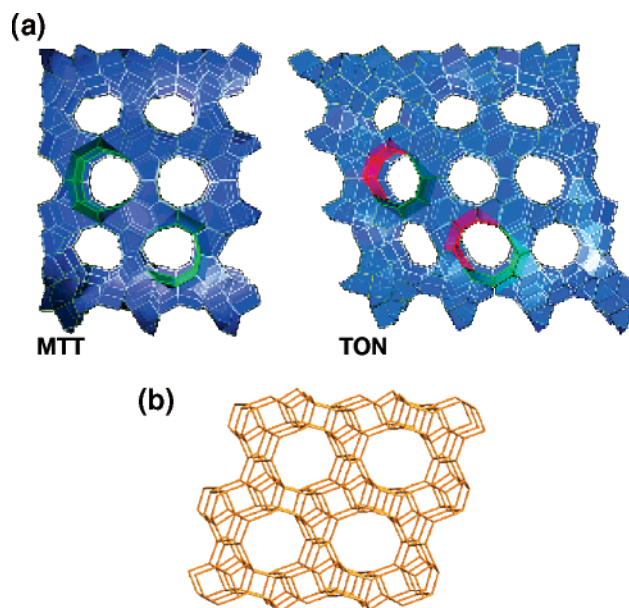


**Figure 2.** (a) Comparison of **MTT** and **TON** frameworks showing large troughs shaded (green in **MTT**, red and green in **TON**). (b) Model of the one-dimensional 12-ring pore framework for ZSM-12 (**MTW**).

commercially available) and examined their structure-directing effects in zeolite syntheses.

This work is a sequel to a study we recently published on the use of diquaternary SDAs based upon imidazolium derivatives.[39] In that work molecular modeling was used to examine the structure-directing effects of imidazolium monomer derivatives as well as their diquaternary analogues in which two imidazole rings were connected by methylene chains of varying carbon lengths. A key point in that investigation was that the isopropyl groups of the DIPI molecule are separated by a distance of 5 Å, equivalent to the periodicity along the pore axis of the **MTT** framework. The isopropyl groups were determined to reside above the corrugations, or troughs, centered within the wider ends of the teardrop-shaped pores (Figure 2). This optimized configuration is verified by a single-crystal XRD study of an as-made sample prepared in fluoride-containing gels.[40] The space above these corrugations allows optimal van der Waals contacts with isopropyl-type groups. Further support for this explanation is that the trimethylammonium groups in the C7 and C11 diquats investigated by Moini[41] are also separated by 10 and 15 Å, distances that are multiples of the periodicity between consecutive troughs. This led us to consider diquaternary molecules in which *N*-isopropylimidazolium groups were connected by methylene chain lengths of five and nine C atoms to give distances between the isopropyl groups of 15 and 20 Å, respectively. However, to this author's disappointment, none of the various conditions of synthesis yielded an **MTT**-type phase. Both diquaternary molecules yielded ZSM-5 in aluminosilicate compositions and Nu-86 in all-silica compositions in concentrated fluoride media. From these results we concluded that although these SDA molecules have good energetic fits within **MTT** pore structure, kinetic rather than thermodynamic effects may be the overriding factor in the phase

(30) Corma, A.; Navarro, M. T.; Rey, F.; Valencia, S. *Chem. Commun.* **2001**, 1720−21.
(31) Rey, F.; Corma, A. Personal correspondence.
(32) Castaneda, R.; Corma, A.; Fornes, V.; Rey, F.; Rius, J. *J. Am. Chem. Soc.* **2003**, *125* (26), 7820−1.
(33) Plank, C. J.; Rosinski, E. J.; Rubin, M. K. U.S. Patent 4,076,842, 1976.
(34) Valyocsik, E. W. U.S. Patent 4,490,342, 1984.
(35) Parker, L. M.; Bibby, D. M. *Zeolites* **1983**, *3*, 8.
(36) Araya, A.; Lowe, B. M. U.S. Patent 4,705,674, 1987.
(37) Zones, S. I. U.S. Patent 5,053,373, 1991.
(38) Nakagawa, Y. U.S. Patent 5,707,601, 1998.

(39) Zones, S. I.; Burton, A. W. *J. Mater. Chem.* **2005**, *15*, 4215−4223.
(40) Zones, S. I.; Darton, R. J.; Morris, R.; Hwang, S.-J. *J. Phys. Chem. B* **2005**, *109* (1), 652−661.
(41) Moini, A.; Schmitt, K. D.; Valyocsik, E. W.; Polomski, R. F. *Zeolites* **1994**, *14*, 564.
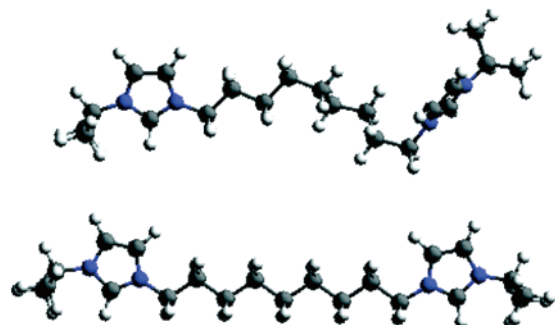
**Figure 3.** Comparison of two conformations of 1,9-bis(isopropylimidazolium)nonane. The top conformation possesses slightly lower energy than the bottom one.

selectivity. Another consideration is that both sets of imidazole rings and isopropyl groups must be perfectly aligned to allow an optimal fit within the one-dimensional **MTT** pore. There are several conformations of the diquaternary molecules that have nearly the same or even less internal energy than the straight chain conformation required for occlusion of the molecule within the pore space (see Figure 3). At typical synthesis conditions it is probably entropically difficult for the molecule to have the necessary conformation for occlusion within the **MTT** structure. This suggested that molecules without the rigid rings may be more suitable candidates.

## II. Experimental Section

**Zeolite Syntheses.** Unless otherwise stated with the text, zeolite syntheses using neutral amines were performed with gels of the following composition: 0.10 $K_2O$:0.20 SDA:1.0 $SiO_2$:0.008, 0.015, 0.033 $Al_2O_3$:42 $H_2O$. Cabosil M-5 was used as the silica source, and Reheis F-2000 aluminum hydroxide was used as the aluminum source. In a few examples zeolite Y (LZY-52) was instead used as the aluminum source. For the borosilicate syntheses with neutral amines, the typical gel composition was 0.05 $K_2O$:0.40 SDA:1.0 $SiO_2$:0.017 $B_2O_3$:42 $H_2O$. Potassium tetraborate decahydrate was the boron source in these syntheses.

For the quaternary ammonium molecules most syntheses were performed with the SDA in the halide form. The all-silica syntheses typically were performed with $OH/SiO_2$ ratios between 0.15 and 0.20. The aluminous gels required higher hydroxide concentrations (0.25−0.30). In one instance (for Molecule O), the high alkali concentration in the aluminosilicate gels resulted in a layered phase. For this example the SDA was ion-exchanged into the hydroxide form by dissolving it in water and adding it to a 5-fold excess of Biorad AG 1-X8 exchange resin. After 24 h, the exchange resin was removed by filtration, and the hydroxide concentration of the SDA solution was determined by titration with a standard solution of 0.1 N HCl. The gel components for the zeolite syntheses were mixed together in 23 mL Teflon liners that were then sealed and placed inside steel Parr autoclaves. These were then inserted into a rotating spit (43 rpm) inside an oven at a fixed temperature (150−170 °C) for 5−30 days. Most syntheses were performed at 160 °C. In general, the all-silica and borosilicate syntheses required 5−8 days of synthesis time, the syntheses with SAR (silica to alumina ratio) = 66 required about 7−10 days, and the syntheses with SAR = 33 required 14−17 days. The syntheses were monitored by periodically performing XRD analyses on small amounts of gel removed from the reactors. The powder XRD measurements were performed with a Siemens D-500 instrument. For each SDA that produced an **MTT** phase, at least two syntheses were performed to check for reproducibility of its structure-directing effects.

**Table 1.** Energy Minimization Calculations for SDA Host Complexes Involving Small Molecules

| SDA | Stabilization MTT (kJmol SDA) | TON (kJ/mol SDA) | MTW (kJ/mol SDA) | Stabilization MTT (kJ/mol T Atom) | TON (kJ/mol T Atom) | MTW (kJ/mol T Atom) |
|---|---|---|---|---|---|---|
| N (trimethylamine) | -83.32 | -52.85 | -72.40 | -6.94 | -4.36 | -5.17 |
| NH | -67.30 | -63.20 | -55.30 | -5.60 | -5.27 | -3.90 |
| H N (ring) | -81.90 | -67.50 | -82.70 | -6.83 | -5.62 | -5.90 |
| NH₂ | -63.32 | -12.70 | -86.10 | -5.27 | -1.06 | -6.15 |
| N+ | -29.90 | -4.23 | -80.18 | -2.50 | -0.35 | -5.73 |
| NH₂ | -65.55 | -26.61 | 81.71 | -2.73[a] | -1.11[a] | -5.84 |

[a] Two unit cell along pore direction.

**Molecular Modeling.** Molecular modeling simulations were performed with the Cerius2[42] software. The reported stabilization energies are differences in energy of the optimized free molecule and the molecule occluded within the zeolite framework. Contributions from van der Waals interactions, valence bond, angle, and torsion energies were determined with the combination of the Burchart and Universal force fields.[43] The positions of framework atoms were fixed during the energy minimizations, and Coulombic interactions between the cation and the zeolite framework were neglected. At least 15 different configurations of the SDA were sampled for each framework by (1) placing the molecule in random locations within the void space of the zeolite and (2) changing the initial torsional angles of appropriate functional groups or chains within the SDA molecule. Since in a few cases the length of the SDA is greater than or nearly equal to the length of the unit cell dimension along the pore axis, a supercell was created (as necessary) from multiple unit cells along the one-dimensional pore axis in order to allow adequate space for each molecule. The energy reported for each SDA/framework pair is the minimum found among the configurations sampled.

## III. Results

**Modeling/Synthesis Results with Small Molecules.** The first part of this study examines small molecules that fit within a single unit cell along the pore axis. Table 1 shows the results of the energy minimization calculations for these molecules in three different one-dimensional zeolites that are commonly observed phases in syntheses with molecules of similar dimensions: **MTT**, **TON**, and **MTW**. **MTT** and **TON** are zeolite frameworks with one-dimensional medium pores. The **MTW** framework has one-dimensional large pores. Note that the entries in the left half of the table are the absolute stabilization energies of each molecule, while the entries in the right half normalize those values according to the number of tetrahedral (T) atoms in the unit cell or supercell. The latter numbers are the better basis of comparison since they provide relative quantitative evaluations of *how the silica is stabilized* for each of the frameworks.

The first entry for trimethylamine shows a very favorable stabilization of −6.9 kJ/mol T atom in the **MTT** framework.

(42) *Cerius2 Modeling Environment, Release 4.8*; Accelrys Software Inc.: San Diego, 2005.
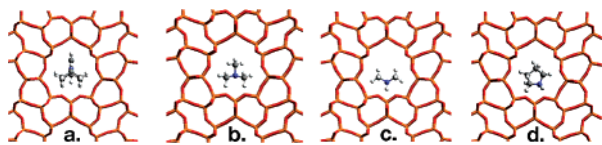(43) de Vos Burchart, E. Ph.D. Thesis, Technical University of Delft, The Netherlands, 1992; Table I, Chapter XII.

**Figure 4.** Cross-sectional views of the energy-optimized positions of (a) DIPI, (b) trimethylamine, (c) dimethylamine, and (d) pyrrolidine.

Figure 4a,b compares cross-sectional views of the positions of the DIPI molecule and the trimethylamine molecule within the **MTT** pore. The size and shape of both molecules are nicely reflected in the dimensions and shape of the **MTT** pore. Pyrrolidine is another molecule that possesses a very favorable energetic fit within the **MTT** pore (Figure 4d). Removal of a methyl group (Figure 4c, dimethylamine) reduces the stabilization in **MTT** to $-5.6$ kJ/mol T atom, a still very favorable energy. However, note that the **TON** framework has a nearly equivalent energy of $-5.3$ kJ/mol T atom. The researchers at Mobil also showed a nearly equivalent stabilization in **MTT** and **TON** for the ethylamine molecule, which has a backbone structure identical to dimethylamine.[44] We need to keep this in mind as we consider the synthesis results for this molecule. The lesson here is that each methyl moiety in the trimethylamine molecule provides significant stabilization in the **MTT** pore. However, when *tert*-butylamine is considered, the larger pore dimensions of **MTW** are calculated to give a better fit. In this case, steric repulsions between neighboring molecules slightly reduce the stabilization within the **MTT** pore. In its energy-optimized position a slight adjustment in the position of the molecule or exchanging the position of the amino group for a methyl group results in substantial decreases in the stabilization. An interesting difference is observed with the tetramethylammonium molecule. Although this molecule has the same backbone structure as *tert*-butylamine, its stabilization is calculated to be less than one-half that of *tert*-butylamine. The space required by the extra proton further increases the steric repulsions between adjacent molecules located within the same pore.

When the backbone of the molecule is again extended to give neopentylamine, the molecule is now too large to fit within one unit cell of both the **MTT** and **TON** frameworks without suffering severe steric repulsions from neighboring molecules. In this case a supercell two unit cells in length must be chosen for those frameworks, and only one-half of the large troughs in the **MTT** framework are stabilized by van der Waals contacts with either an isopropyl- or *tert*-butyl-type group. Here the 12-ring pore of **MTW** is calculated to give a more favorable fit.

Table 2 gives the results of our syntheses with some of these small molecules at SAR gel ratios of 33 and 66. Note that the first two entries, trimethylamine and isopropylamine, have identical backbone structures and that they each yield the same results. At SAR ratios of 33 and 66, the experimental results are **MFI** and **MTT**, respectively. Although trimethylamine has a very good energetic fit within the **MTT** pore structure (greater than more selective molecules as we will discuss later), it is only selective for **MTT** at the higher SAR ratio. Nonetheless, the calculations successfully indicate that **MTT** should be a preferred phase using these molecules as SDAs. It is worth

(44) Rollmann, L. D.; Schlenker, J. L.; Lawton, S. L.; Kennedy, C. L.; Kennedy, G. J.; Doren, D. J. *J. Phys. Chem. B* **1999**, *103* (34), 7175–7183.

**Table 2.** Phase Selectivity For Syntheses with Small Amines[a]

| SDA | SAR = 33 | SAR = 66 |
|---|---|---|
| trimethylamine | MFI | MTT/Minor Cristobalite |
| isopropylamine | MFI | MTT |
| dimethylamine | Amorphous | Amorphous - SSZ-54[b] in one case |
| pyrrolidine | MTT | MTT |
| (NH2) | Cristobalite/Minor MTT- 23 Days | MTT/MFI Cristobalite |
| (NH2) | Amorphous | Layered |
| (N-H) | Amorphous | Layered |
| (NH2) | TON | TON |
| (NH2) | Amorphous | Amorphous |

[a] SAR = $SiO_2/Al_2O_3$. [b] Intergrowth of **MTT** and **TON**.

pointing out that although trimethylamine has been previously reported to promote the synthesis of **MTT**, the person who performed these calculations was then unaware of that result and therefore was able to provide an unbiased assessment of the potential structure-directing ability of that molecule.

In the experiments of the current work dimethylamine yielded only amorphous products at the low SAR, and in most cases an amorphous product was also obtained at the higher SAR ratio. However, in one trial SSZ-54 an **MTT**/**TON** intergrowth (vide infra) was observed. It is interesting to note that the calculated stabilizations of dimethylamine are similar in the **MTT** and **TON** frameworks. Parker and Bibby prepared an **MTT** phase using dimethylamine in gels where the SAR ratio was about 110. We are able to reproduce their synthesis using $Al_2(SO_4)_3$ as the aluminum source, although our experiments require 7–9 days rather than the previously reported 40 h. While dimethylamine does have a favorable fit in the **MTT** pore structure, its weaker selectivity for **MTT** (over a wide range of SAR values) may be a reflection of the relative stabilizations of trimethylamine and dimethylamine.

*tert*-Butylamine was slow to crystallize any products at SAR = 33. Only a minor amount of **MTT** crystallized after 23 days, and the rest of the product was mostly cristobalite. Seeding changed neither the crystallization rate nor the phase selectivity. At SAR = 66, use of *tert*-butylamine yielded comparable quantities of **MTT** and cristobalite as estimated by powder XRD. These results are interesting when interpreted within the context of the energy optimizations performed for this molecule. Recall that although the molecule has a favorable fit within the pore, the calculations indicate the molecule has little freedom of rotation or orientation without encountering steric repulsions from its nearest neighbors. The difficulty in crystallizing **MTT** may be a reflection of these observations. Another point worth consideration is that **MTW** is not formed with this molecule although it is calculated to have a better fit. In our group's work

**MTW** phases are rarely crystallized using neutral amines as SDA although quaternary ammonium compounds with similar size frequently yield **MTW** phases. It should also be recognized that this molecule is small enough to pass freely through the **MTW** pores with little energetic barrier. This could adversely affect the ability of the molecule to either nucleate this phase or prevent its dissolution.

Neopentylamine and *N*-methyl-*tert*-butylamine each gave only amorphous or layered products in our syntheses. These molecules are unable to provide significant stabilization to the **MTT** framework since only one-half of the troughs can be "occupied" by an isopropyl- or *tert*-butyl-type group. Again, these molecules have favorable stabilization energies within the **MTW** framework, but they also have easy egress from the pores.

The last two molecules in Table 2, 1-methylbutylamine and 3-methylbutylamine, have equivalent backbone structures defined by the connectivity of the carbon and nitrogen atoms. However, while 1-methylbutylamine yields **TON** in both SAR conditions, 3-methylbutylamine yields no crystalline products. Here the idea fails that molecules that possess equivalent backbone structures should yield similar phases in their syntheses. Several molecules have been reported to crystallize **TON** zeolites.[45,46] Many of them either are completely linear molecules or possess a single methyl branch. Outside these observations we have been unable to find any unifying characteristics of molecules that promote crystallization of **TON** zeolites. As discussed in the Introduction, it is easier to "design" an SDA for a particular zeolite phase that has salient features such as a cage or periodically spaced channel intersections. The **TON** framework has no such prominent features. The following sections will discuss several molecules that have been chosen by design as SDAs for **MTT**. These considerations take advantage of large troughs present in the **MTT** pores and the periodicity between them.

**Synthesis of Amines for This Study.** While some of the molecules examined as SDAs in this study are commercially available chemicals, many of the amines had to be synthesized in the laboratory. Two routes were used to prepare the novel amines. One method simply involves a one-step alkylation of an amine with an alkyl halide. Figure 5a shows an example of the synthesis of *N*-isopropyl-*N*-isoamylamine by this route.

The syntheses of other amines involved bulky functional groups that react slowly in alkylation reactions. Also, the syntheses of some of the diamines in these studies require that each nitrogen atom in the parent diamine be alkylated only once. In typical reactions with alkyl halides, it is possible that the nitrogen atom may be alkylated multiple times if the product remains in solution. To avoid these problems, the parent amine or diamine was reacted with an appropriate acid chloride. The amide products were then reduced with LiAlH$_4$ to obtain the desired product. Figure 5b shows the synthesis scheme and $^1$H NMR of *N*,*N*′-diisobutyl-1,3-propanediamine obtained by this technique. The Supporting Information describes the synthesis of each novel molecule.

**Synthesis Results for Molecules with 5 Å Repeat Between Branched Groups.** The results for the molecular modeling of the DIPI molecule[39] indicate that isopropyl-type groups prefer
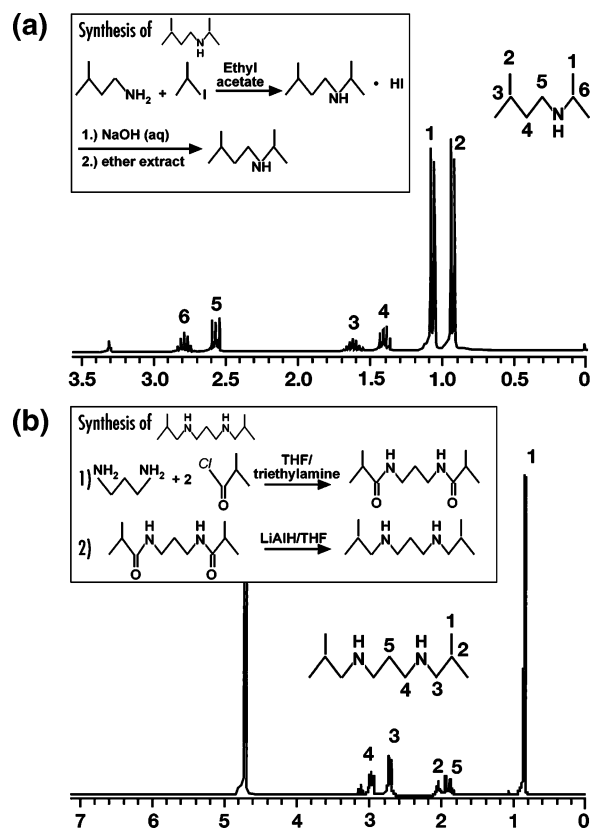


***Figure 5.*** (a) Synthesis scheme and $^1$H NMR of *N*-isopropyl, *N*-isoamylamine. (b) Synthesis and $^1$H NMR of diamine in *d*-MeOH.

to reside above the troughs within the **MTT** pores. This suggests that molecules that have terminal isopropyl groups separated by 5 Å, equivalent to the distance between the centers of these troughs, may be ideal candidates for the synthesis of **MTT** zeolites. Another requirement is that the terminal groups must be connected by a group that is narrow enough to fit within the constrictions of the **MTT** pore. For the DIPI molecule, the imidazole ring is an ideal fit within these pore constrictions. Functional groups with larger cross sections will not fit. We will examine molecules where the branched groups are connected by either linear alkyl chains or linear chains in which an amino group is substituted for a methylene unit. As discussed in the previous study on imidazolium diquaternary molecules,[39] the distance between every other carbon atom in a straight alkyl chain is about 2.5 Å. This distance changes very little if a nitrogen atom is substituted for one of the methylene carbon atoms. Therefore, if there are three "backbone" atoms connecting two isopropyl centers, then the distance between the centers will be 5 Å.
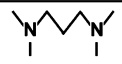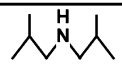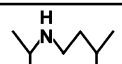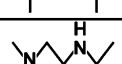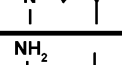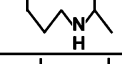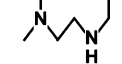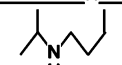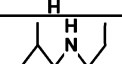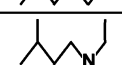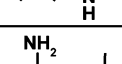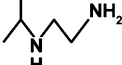
The first four molecules in Table 3 meet the description given above. Note that the first two molecules are selective for **MTT** at both SAR ratios. However, molecules C and D both give **MFI** at SAR = 33 and **MTT** at SAR = 66. Surprisingly, when **MTT** seeds are used with molecule C (0.02 g of seeds per 0.90 g of Cabosil) for SAR = 33, the phase selectivity is altered to **MTT**. Moreover, when zeolite Y is used as the aluminum source in gels with SAR = 33 and *without seeds*, **MTT** is again the preferred phase for molecule D.

These are interesting results when considered in the context of the relative nucleation rates of these phases in gels with high aluminum concentrations. Zeolite phases with lower framework

(45) Szostak, R. *Handbook of Molecular Sieves*; Van Nostrand Reinhold: New York, 1992.
(46) Gies, H.; Marler, B. *Zeolites* **1992**, *12*, 42.

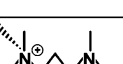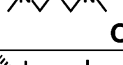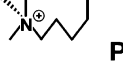**Table 3.** Phase Selectivity Observed for Molecules with Branch Groups Separated by 5 Å[a]

| SDA | SAR = 33 | SAR = 66 |
|---|---|---|
| A | MTT | MTT |
| B | MTT | MTT/Minor Cristobalite |
| C | MFI MTT w/seeds | MTT |
| D | MFI MTT w/NaY | MTT |
| E | MTT | MTT |
| F | MFI | MTT |
| G | MFI | MTT > MFI |
| H | MFI | MFI > MTT |
| I | MFI | MFI |
| J | MFI | SSZ-54 |
| K | MFI | SSZ-54 |
| L | Amorphous | Cristobalite |
| M | Amorphous | Cristobalite |

[a] SAR = $SiO_2/Al_2O_3$.

**Table 4.** Phase Selectivity for Quaternary Amines with Branched Groups Separated by 5 Å

| SDA | SAR = 33 | SAR = 66 | All Silica | SBR = 66 |
|---|---|---|---|---|
| O | MTT OH/$SiO_2$=0.25 | MTT OH/$SiO_2$=0.25 | MTT/Crist 7 days OH/$SiO_2$=0.20 | MTT/Minor quartz |
| P | MFI after 25 days OH/$SiO_2$=0.30 | MFI after 7 days OH/$SiO_2$=0.25 | MTT/Minor MTW -7 days OH/$SiO_2$=0.15 | MFI after 7 days OH/$SiO_2$=0.25 |
| R | MFI after 7 days OH/$SiO_2$=0.30 | MFI after 7 days OH/$SiO_2$=0.25 | ZSM-48 after 7 days | MFI after 7 days OH/$SiO_2$=0.15 |
| S | Amorph. after 25 days OH/$SiO_2$=0.30 | Amorph. after 1 month OH/$SiO_2$=0.25 | ZSM-48 after 7 days OH/$SiO_2$=0.15 | ZSM-48 after 7 days OH/$SiO_2$=0.15 |

densities are often favored in gels with higher aluminum content. ZSM-5 can be synthesized in the presence of a large number of amines, although many of them do not have an exceptional energetic fit within the **MFI** framework. Good examples are the data for isopropylamine and trimethylamine in Table 2. These results are consistent with ZSM-5 being a more kinetically favored phase when aluminum is present in high concentration. By using seeds in the case above we are able to circumvent this problem by providing nucleation centers from the outset. Also, by using zeolite Y as an aluminum source we limit the concentration of reactive aluminum immediately available to the rest of the gel. However, it is important to point out that use of seeds or zeolite Y as an aluminum source does not change the phase selectivity for all of the SDA molecules that produce **MTT** only at the low aluminum conditions.

The second group of molecules (E–J) in Table 3 is similar to the first set with the exception that a single methyl group has been removed from one of the terminal isopropyl-type moieties. Removal of a methyl group effectively reduces the stabilization afforded by an isopropyl group above the pore corrugations in the **MTT** pores. We therefore might expect this group of molecules (collectively) to show less selectivity for **MTT**. E is surprisingly selective for **MTT** at both SAR

conditions. F–J yield different results. They all yield **MFI** at SAR = 33. *N*-Isoamyl-*N*-ethylamine (I) gives **MFI** for the higher SAR. However, it is necessary to point out that *N*-isobutyl-*N*-propylamine (H) and *N*-isopropyl-*N*-butylamine (G) both give a mixture of **MFI** and **MTT** at SAR = 66. We next repeated syntheses at SAR = 120 to determine if the phase selectivity for this group of molecules could be shifted toward **MTT**. For this SAR, H and I both gave a pure **MTT** phase, G gave an **MTT/TON** intergrowth, and J gave **TON**. Within this collection of molecules it is interesting to note that the lower stabilization of the SDA (through removal of a single methyl group) is reflected in the weaker selectivity for **MTT**. It is also noteworthy that the two diamines in this group both show good selectivity for **MTT** despite removal of the methyl group. Although there is no current explanation for their better selectivity, it is tempting to believe it is related to the presence of the two amino groups.
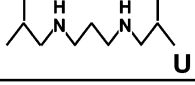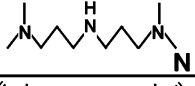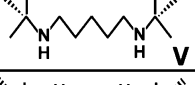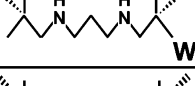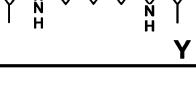
Molecule K yields SSZ-54,[47] an **MTT/TON** intergrowth. The synthesis and structure of this material will be discussed in a future publication.

The last two molecules (L, M) in Table 3 are similar to the first group except that an extra methyl group has been added to one of the central atoms of the terminal branched group to create a "*tert*-butyl-type" functional group. The synthesis results for these molecules are very intriguing. We performed energy minimizations for *N*,*N*,*N*,*N*′,*N*′-pentamethyl-1,3-propanediamine (Molecule O in Table 4) within the **MTT** framework. The asymmetry of the molecule allows two possible local configurations of the molecule within the **MTT** framework: one in which the "*tert*-butyl" ends on adjacent molecules directly face each other, and one in which the "*tert*-butyl" groups face away. The second configuration gives a favorable stabilization of −5.7 kJ/mol T atom, while the first gives only −1.7 kJ/mol T atom. Molecules L and M possess the same backbone structure as this molecule, yet the syntheses with these molecules yielded only amorphous or dense phase products (in one experiment minor **MTT/MFI** was detected by XRD). These results are different from their quaternary analogue (Table 4).

Molecule O is selective for **MTT** at all synthesis conditions examined including the all-silica synthesis and the borosilicate synthesis (SBR = 66). This high selectivity is consistent with the calculated stabilization mentioned above. The lack of

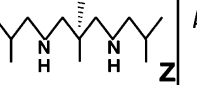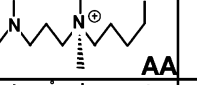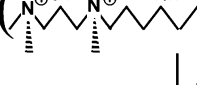(47) Zones, S. I.; Burton, A. W. U.S. Patent 6,676,923, 2004.

**Table 5.** Phase Selectivity for Molecules with Branched Moieties Separated by Multiples of 5 Å

| SDA | SAR = 33 | SAR = 66 | SBR = 66 |
|---|---|---|---|
| (structure) T | MFI | MTT | MTT |
| (structure) U | MFI | MTT | MTT |
| (structure) N | MFI | SSZ-54 | TON |
| (structure) V | MFI | MTT | MTT |
| (structure) W | Amorph./Trace MFI | Amorph. | Amorph. |
| (structure) X | MTT | MTT | Kenyaite |
| (structure) Y | MFI | MTT | MTT |

**Table 6.** Other Interesting Candidate Molecules for **MTT**-type Zeolites

| SDA | SAR = 33 | SAR = 66 | All Silica | SBR = 66 |
|---|---|---|---|---|
| (structure) Z | Amorph. | Crist./MTT/Amo. after 7 days. | – | – |
| (structure) AA | MFI | MFI | MTT | MFI |
| (structure) BB | MTT | MTT | MTT | MTT/minor MTW |
| (structure) CC | MTT | MTT | ZSM-48 | MTW |
| (structure) DD | MTT | MTT | Crist. | MTT (SBR 33) |
| (structure) EE | Amorph. | MTT/Minor Crist. | MTT | MTT |

selectivity observed in its isostructural compounds (L and M) is not consistent with our predictions. This may be due to the weak polarity of these molecules since the nitrogen atoms are unquaternized, the C/N ratio (9) is high, and the nitrogen atoms are close to *tert*-butyl groups. If we now consider a compound in which a single methyl group is removed from one of the branched groups (P), we should expect a weaker selectivity for **MTT**. In fact, this compound yields **MTT** only in the all-silica case. Note that addition of another methylene carbon to the backbone structure (R) creates a compound that does not give **MTT** under any synthesis conditions.

**Synthesis Results for Molecules with Multiples of 5 Å Between Branched Groups.** Table 5 shows diamines with isopropyl or *tert*-butyl groups separated by 10 or 15 Å. The first two molecules differ only in the positions of the nitrogen atoms within the connecting chains. In both cases, **MFI** and **MTT** are the preferred phases at SAR = 33 and 66, respectively. However, molecule N unexpectedly gives an **MTT/TON** intergrowth at SAR = 66. Intuitively, we expect these molecules to show weaker selectivity than the first group of molecules in Table 3 since only every other trough in the **MTT** pore may be occupied by a branched moiety. Molecules V and W are analogous to the first pair except that *tert*-butyl groups are substituted for the isopropyl groups at the ends of each molecule. Although V has the same phase selectivity as T and U, W does not promote crystallization of **MTT** under any conditions with or without seeds. However, we observed that this molecule is not soluble in water, and after the synthesis mixture was removed from the oven the organic amine appeared as a separate layer above the rest of the gel. The organic layer was verified by NMR to be the original SDA. Its insolubility may explain its lack of structure-directing ability. The last diamine (Y), with terminal isopropyl groups separated by 15 Å, also yields **MTT** at SAR = 66.

**Synthesis Results For Oligomeric or Polymeric Molecules with Multiples of 5 Å Between Branched Groups.** Table 6 shows molecules that are oligomeric in the sense that there are multiple pairs of branched dimethyl groups separated by 5 Å. The phase selectivities of molecules AA and BB mirror those of P and O, respectively. Both BB and O are selective for **MTT** in every condition we examined, but, once again, if a terminal methyl group is removed (AA), the SDA crystallizes **MTT** only in the all-silica composition and **MFI** in the aluminosilicate and borosilicate compositions. The triquaternary SDA CC is similar to the C7-TMA-diquat (X) except that a dimethylammonium center has replaced the middle carbon atom in the methylene chain, thereby creating a molecule with three charged nitrogen centers separated by 5 Å. This molecule has been previously reported by Mobil as an SDA for ZSM-23.[48] Molecule CC promotes crystallization of **MTT** phases over a wide range of Si/Al ratios, but interestingly its phase selectivity switches to **MTW** (a one-dimensional 12-ring zeolite) in the borosilicate gel. Also, unlike the diquat, this molecule gives ZSM-48 in all-silica syntheses. The charge density of this molecule would demand a high concentration of silanol defects in an all-silica zeolite. These defects destabilize zeolite frameworks relative to their fully intact structures.[17,49] It is possible that the framework of ZSM-48, which is frequently observed in all-silica compositions with a variety of linear molecules, is better able to accommodate the required defect density because it possesses an inherently more stable framework than **MTT**.

The last two molecules are polycationic polymers with (1) repeat distances of 5 Å and (2) alternating repeat distances of 5 and 10 Å between the quaternary centers. The polymers are a significant test of the premise we established because, like the zeolite structure itself, these SDA molecules possess periodically spaced units. Polymer EE is selective for **MTT** over

(48) Moini, A. U.S. Patent 5,332,566, 1994.
(49) Burton, A.; Zones, S.; Elomari, S. *Curr. Opin. Colloid Interface Sci.* **2005**, *10*, 211.

a wide range of compositions except at SAR =33. However, DD (like CC) does not yield **MTT** in the all-silica compositions, and a higher concentration of boron (SBR = 33) is required to give an **MTT** phase without significant cocrystallization of dense phases. Nonetheless, the phase selectivities of the larger molecules in this section are consistent with the empirical rules we established for the design of **MTT**-specific SDA (although the compositional requisites of the gels may vary for individual SDA molecules).

Molecule Z was not an effective SDA for any zeolite phase. As in Molecules L and M, the nitrogen atoms in this molecule are surrounded by bulky groups that may increase the hydrophobic character of the molecule. However, in a few of the preparations a minor **MTT** phase was detected.

**Characterization of MTT Phases and Pore-Filling Effects.** Supporting Information Figure 1 shows characteristic powder XRD patterns for the **MTT** phases prepared with each of the SDA molecules in the study. In a few products cristobalite is present (peak at 22° 2$\theta$), but the samples are otherwise free of detectable impurities. Supporting Information Table 1 shows the Si/Al ratio, K/Al ratio, CHN content, and pore filling for the **MTT** zeolites crystallized from selected SDA compared with theoretical values based upon optimal packing arrangements of that molecule. The C/N ratios of the as-made zeolites are close to those expected for their respective SDAs. Note that, in general, for syntheses involving unquaternized amines the preparations with high Si/Al ratios give products where the SDA fills 90−100% of the expected space available within the micropores. The maximum capacities are based upon the packing arrangement that gives the best fit of each molecule within the framework. In contrast, the preparations with higher aluminum contents yield products with only 80−90% of the maximum capacity. How do we explain this difference?

We expect the more aluminous zeolites to have higher concentrations of extraframework potassium for charge compensation. Since there are no isolated cages in the **MTT** framework within which potassium cations may reside (except perhaps within the six rings), many of these potassium cations will occupy space within the pores that otherwise would be filled by an SDA molecule. A slightly smaller organic content is therefore anticipated for zeolites with more extraframework alkali cations. The only samples that significantly fall short of their maximum pore-filling capacities are those prepared with isopropylamine (50%) and trimethylamine (34%). (It should be noted that the **MTT** phase produced with trimethylamine contained cristobalite impurity.) Given the excellent fits of these two molecules within the **MTT** pore space, it is difficult to rationalize why no more than one-half of the internal troughs are occupied by the SDA. If the amines are occluded primarily in their protonated forms, then a higher concentration of SDA molecules requires more framework charge than can be provided by the available aluminum. This supposition is supported by a previous Mobil study of small amines in zeolite synthesis.[44] Although the stabilization provided by van der Waals contacts is reduced by the lower SDA loading, the defects required for charge compensation (of a higher concentration of protonated SDA) destabilize the framework to a greater extent.

Another interesting result, however, is the variance of K/Al ratio observed among the different samples. For example, the K/Al ratios for diisobutylamine are 0.94 and 0.48 in the preps

with SAR of 33 and 66, respectively. In one case nearly all of the extraframework charge is accounted for by potassium, and in the other only one-half of the charge is accounted for by potassium. By examining the data for the other SDAs it can be seen that a 1:1 ratio of K/Al is the exception rather than the rule. How do we account for the remaining charge? Previous NMR studies by Hwang and Zones indicated that in SSZ-25 samples prepared in the presence of both *N,N,N*-trimethyl-2-adamantammonium and isobutylamine isobutylamine was occluded with the framework as a protonated molecule. The Mobil study also strongly suggests a large fraction of occluded amines are protonated.

**Borosilicate Syntheses of MTT Phases.** One of the surprising findings in our initial studies was that **MTT** phases were rarely observed to crystallize from borosilicate gels in syntheses with unquaternized amines. The neutral amines gave either dense or layered phases with $KOH/SiO_2 = 0.2$. Dense or layered phases often crystallize when the hydroxide or alkali concentration is too high. A series of experiments were performed in which the $KOH/SiO_2$ ratio was incrementally decreased and the $SDA/SiO_2$ ratio was incrementally increased.

When the $OH/SiO_2$ ratio was decreased to 0.10 with $SDA/SiO_2 = 0.4$, pure **MTT** phases crystallized with several of the diamine molecules. Compound Y crystallized a borosilicate **MTT** phase (gel Si/B = 33) after 16 days of heating at 160 °C. A, D, E, and F usually crystallized an **MTT** phase within 7 days. E was particularly successful in crystallizing **MTT** phases. This molecule produced borosilicate **MTT** phases after 6−7 days of heating. With seeds the crystallization time could be reduced to 3 days with this SDA. Molecule A crystallized **MTT** in 4 days with the use of seeds. However, the monoamine molecules (including isopropylamine, isobutylamine, or diisobutylamine) were never able to crystallize an **MTT** phase.

Next a series of experiments was performed in which the Si/B ratio was systematically varied in gels with molecule E. Pure **MTT** phases crystallized from gels with Si/B ratios as low as 5. However, the concentrations of boron in the products were significantly lower, an indication of the solubility of boron in contrast to aluminum. For gels with Si/B ratios of 32, 16, and 5, the respective product ratios were 49, 34, and 23. It should be noted that the boron content was increased by adding potassium tetraborate and that no decreases were made in the amount of KOH added to the gel. The effective $K_2O/SiO_2$ gel ratio therefore also increased when the boron concentration was increased.

The lower alkali hydroxide content necessary for successful preparations of borosilicates (with neutral amines) was an initial surprise. In our group's experience with quaternary ammonium molecules as SDA, borosilicate zeolites are often prepared with alkali hydroxide contents that are similar to those we use for aluminosilicates. However, examination of the work by Gies and co-workers[50−54] and the group at EniTecnologie[55] reveals that many of their borosilicate syntheses are carried out with high concentrations of amines and with little or no alkali

(50) Marler, B.; Gies, H. *Zeolites* **1995**, *15*, 517.
(51) Vortmann, S.; Marler, B.; Gies, H.; Daniels, P. *Microporous Mater.* **1995**, *4*, 111.
(52) Vortmann, S.; Marler, B.; Daniels, P.; Dierdorf, I.; Gies, H. *Stud. Surf. Sci. Catal.* **1995**, *98*, 262.
(53) Grunewald-Luke, A.; Gies, H. *Microporous Mater.* **1994**, *3*, 159.
(54) Gies, H.; Gunawardane, R. P. *Zeolites* **1987**, *7*, 442.
(55) Millini, R.; Perego, G.; Bellussi, G. *Top. Catal.* **1999**, *9*, 13−34.

**Table 7.** Synthesis Results for Amines or Quaternary Ammonium Compounds That Do Not Possess Multiples of 5 Å Between the Isopropyl, Dimethylamino, or Trimethylammonium Groups

| SDA | SAR = 33 | SAR = 66 | SAR >1000 |
|---|---|---|---|
|  | Layered | Layered | – |
|  | Amorph. | Layered | – |
|  | MFI | TON | – |
|  | MFI | MFI/Cristobalite | – |
|  | Crist./MTT/ MFI/Layered | MTT | ZSM-48 |
|  | Layered | MTT | ZSM-48 |

**Table 8.** Measured C/N Ratio of Zeolite Products for SDA That Unexpectedly Yield an **MTT** Phase

| SDA | Measured C:N of Product |
|---|---|
|  | 8.0 |
|  | 4.7 |
|  | 5.8 |
|  | – |

hydroxide. A low alkali hydroxide content may be necessary to allow a sufficient concentration of protonated amines to exist in the borosilicate gel mixture. The studies by Zones and Hwang and by the Mobil group suggest that a significant portion of occluded amines is in a protonated form. These observations and the fact that quaternary ammonium molecules successfully crystallize zeolites at high hydroxide conditions indicate that the presence of the cationic SDA may be necessary for nucleation of the zeolite. It was noted earlier that many of the diamines in this study were successful in crystallizing borosilicate **MTT** while the monoamines were not. Perhaps this is because the polyamines molecules are more likely to exist as protonated species.

However, why do amines seem to work well with high hydroxide conditions in aluminosilicate compositions? Aluminosilicate gels are not as soluble as borosilicate gels in hydroxide media. The aluminosilicate gels are therefore slower to convert to dense phases. The extended time for crystallization may allow a larger number of protonated amines to be "trapped" by silicate species during the nucleation stages.

**Syntheses with Molecules without Multiples of 5 Å Between Branched Groups and Exceptions to the Rule.** To test the consistency of the empirical rules that have been established in identifying SDA selective for **MTT** phases, it is also important to examine similar SDA molecules with distances between isopropyl, dimethylamino, or trimethylammonium centers that are not multiples of 5 Å. The first four molecules in Table 7 do not crystallize **MTT** phases under any of the conditions we examined. However, contrary to our predictions, the C8 and C12 trimethylammonium diquats succeed in crystallizing **MTT** phases at SAR = 66. These results are consistent with the previous Mobil studies for SAR = 90. In the all-silica case, both SDA yield ZSM-48; and for SAR = 33, the synthesis with the C12 diquat results in a layered phase, and the C8 diquat yields a mixture of cristobalite, **MTT**, **MFI**, and a layered phase after more than 1 month of crystallization. CHN combustion analyses of the as-made **MTT** products show that the C:N:H ratios of the occluded organic are consistent with the parent

SDA. Therefore, degradation products (such as trimethylamine) are not responsible for crystallization of the **MTT** phase.

Although these diquaternary SDA are exceptions to the empirical rules, it is interesting to compare their phase selectivities with those for the C7 and C11 analogues. The latter molecules possess distances of 10 and 15 Å, respectively, between the trimethylammonium centers. In contrast to the C8 compound, the C7 diquat is able to direct the crystallization of **MTT** both for the all-silica condition and for SAR = 33. Likewise, the C11 diquat is able to crystallize an **MTT** phase at SAR = 33 with only a minor amount of layered impurity phase. The C7 and C11 diquats therefore show greater selectivity for **MTT** than their C8 and C12 counterparts. The interpretation of this author is that because the C7 and C11 provide better fits within the **MTT** pore structure, they are able to direct the crystallization of **MTT** phases over a wider range of conditions.

In examining our research group's database of synthesis results other molecules were found that unexpectedly gave **MTT** phases. Table 8 shows examples of such putative SDA molecules. In the many synthesis trials performed with each molecule, only a single experiment yielded an **MTT** phase, and the product was observed after at least 25 days of synthesis. In addition, the product included an appreciable quantity of cristobalite or quartz. Note that these molecules possess trimethylammonium groups. SDA molecules with trimethylammonium groups can degrade through a Hofmann elimination to form trimethylamine (which is capable of directing the crystallization of **MTT**). Table 8 shows the C:N ratio of the as-made **MTT** product for each of these molecules. Note that the C:N ratio of the as-made zeolites is very different from the parent SDA molecules. This strongly suggests that degradation products are responsible for crystallization of **MTT**. C:N data are not available for the fourth molecule, but it should be noted that many of the synthesis trials with this SDA yielded the dense clathrate ZSM-39 (**MTN**). **MTN** phases are frequently observed in zeolite syntheses when SDA molecules with trimethylammonium groups degrade.

Interestingly, the C:N ratio for each of the phases does not equal that for trimethylamine. Although thorough NMR investigations are required to verify this supposition, this author believes that trimethylamine may start the nucleation of the **MTT** phase and that other degradation products may become
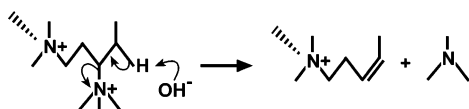
**Figure 6.** Possible Hofmann elimination reaction for the first molecule presented in Table 8.

incorporated within the zeolite during crystallization. The first molecule, however, provides an interesting case where multiple degradation products are capable of forming an **MTT** phase. The measured C:N ratio is 8.0, which is the same as that expected for the first decomposition product shown in Figure 6. This olefinic decomposition product may further react to form an alcohol. Note that this compound has a backbone structure identical to that for molecule P in Table 4. With the exception of a degradation product formed by elimination of both trimethylammonium groups there are no degradation products that have C:N equal to or less than 8. We therefore believe this molecule (or a structurally related alcohol) is the true SDA for the observed **MTT** phase.

## IV. Conclusions

Molecular modeling has been used to investigate the guest/framework van der Waals interactions for small SDA molecules that are known to be specific for **MTT**-type zeolite phases. On the basis of these results and crystallographic considerations of the **MTT** pore structure, several novel molecules have been successfully predicted to be selective for **MTT**. These predictions indicate that amines or quaternary ammonium molecules with isopropyl, dimethylamino, *tert*-butyl, and/or trimethylammonium groups that are separated by multiples of 5 Å and connected by methylene spacers should be able to crystallize **MTT** phases. The predictions are highlighted by crystallization of **MTT** phases using polymeric quaternary ammonium molecules in which dimethylammonium groups are separated by 5 and 10 Å. When a single methyl group is removed from molecules with isopropyl or dimethylamino groups separated by multiples of 5 Å, weaker selectivity is generally observed for **MTT** (e.g., molecules O and P and BB and AA). This reflects a reduced stabilization from the interaction between the SDA and the **MTT** framework.

There are a few exceptions to the rule we established. The C8 and C12 trimethylammonium diquaternary molecules are both one methylene unit longer than preferred distances of 10 and 15 Å, respectively. However, it is noteworthy that both the C7 and C11 diquaternary analogues are selective for **MTT** over a wider range of SAR conditions. This stronger selectivity is probably a manifestation of the better fit these molecules provide within the pore structure. A few molecules were found that produce **MTT** phases although they are too large to fit within the pore structure. These syntheses required at least 25 days, and the CHN combustion analyses indicated the as-made products possess C:N ratios that are very different from the parent SDA. It is proposed that these SDAs degrade to form trimethylamine or other SDAs that may nucleate **MTT** zeolite phases.

Finally, several of the polyamine molecules in this study can be used to prepare borosilicate **MTT** samples. This is the first report of a borosilicate **MTT** phase. The $KOH/SiO_2$ ratio in these gel preparations is at most one-half the hydroxide concentration that we typically use in the crystallization of the aluminosilicate samples ($KOH/SiO_2 = 0.2$) with the same SDA. For the borosilicate preparations, dense or layered phases easily crystallize in gels with higher hydroxide concentrations.

**Supporting Information Available:** Images of all the IZA-coded frameworks discussed in this paper (Appendix 1); XRD of **MTT** with different SDA (Figure 1); pore-filling calculations for the SDA shown (Table 1); list of the SDA (with letter code corresponding to Supplementary Figure 1) with detailed information on synthesis of the amines. This material is available free of charge via the Internet at http://pubs.acs.org.